Dynamic Light Scattering Study of the Effect of Mg^{2+} and ATP on Synthetic Myosin Filaments

Sei-ichi Takayama and Satoru Fujime
Graduate School of Integrated Science, Yokohama City University, 22–2 Seto, Kanazawa-ku, Yokohama 236, Japan

ABSTRACT The dynamic light scattering (DLS) method provides us with information about the apparent diffusion coefficient, D_{app}, as well as the static scattering intensity, I_s, of particles in solution. For long but thin rods with length L and diameter d, the dependence on L and d of D_{app} is quite different from that of I_s. By means of DLS we studied synthetic myosin filaments of rabbit skeletal muscle in solution at pH 8.3 and 10°C. It appeared that Mg^{2+} ions induced thickening and lengthening of the filaments, whereas ATP (and ADP) induced thinning and shortening (depolymerization) of the filaments. When ATP was added to the filament preparation in the presence of Mg^{2+} ions, it was clearly observed that thinning of the filament (or splitting into subfilaments) occurred before shortening (or depolymerization).

INTRODUCTION

Under an appropriate condition, isolated myosin molecules of vertebrate skeletal muscle polymerize into bipolar filaments. In synthetic filaments, the number of myosin molecules per 14.3 nm axial repeat is three (Mochizuki-Oda and Fujime, 1988) to six (for example, Suzuki and Wada, 1981; Persechini and Rowe, 1984) depending on polymerization conditions, whereas in intact filaments this number is three (Maw and Rowe, 1980). Up to now there have been many physico-chemical studies on the architecture of synthetic myosin filaments (for review, see Davis (1988), in which comprehensive references up to 1987 are cited). In one of the earlier studies, depolymerization of synthetic myosin filaments induced by the addition of ATP (ADP, $(PO_4)^{2-}$, etc.) was investigated mainly by measuring the turbidity changes (Harrington and Himmelfarb, 1972). The present study has a deep connection with this study. However, our method of dynamic light scattering (DLS) provides us with information about the diffusion coefficient of the filaments as well as the scattering intensity (which corresponds to the turbidity) from the solution of filaments, allowing us to gain a deeper insight (than in the earlier study) into the architecture of myosin filaments.

The following have been reported from DLS studies of synthetic myosin filaments of rabbit skeletal muscle. (1) At neutral pH, the sizes of I_s (the static scattering intensity) and D_{app} (the apparent diffusion coefficient) are independent of the addition of 5 mM Mg^{2+} and/or 4 mM ATP (Suzuki and Wada, 1981). (2) At an alkaline pH (e.g., pH 8.3), on the other hand, the sizes of both I_s and D_{app} strongly depend on the ionic strength of the solvent (Mochizuki-Oda and Fujime, 1988). (3) At pH 8.3, the size of D_{app} changes with the addition of 3 mM Mg^{2+} (Maeda et al., 1991). We have reconfirmed all of these results cited above and have further studied the effect of Mg^{2+} and/or ATP on the sizes of I_s and D_{app} of myosin filaments at an alkaline pH.

By "ν-filament," we denote a myosin filament consisting of ν subfilaments. Then, the diameter $d(\nu)$ of the ν-filament is given by a relation $d(\nu)^2 = \nu d(1)^2$, because $d(\nu)^2 L$ and $d(1)^2 L$ are, respectively, proportional to the molecular masses of ν- and 1-filaments with length L. In our earlier study by DLS, electron microscopy and analytical centrifugation (Mochizuki-Oda and Fujime, 1988), we have shown that at pH 8.3 the following. (1) Myosin filaments at 1 mM Mg^{2+} and ionic strength of 134 mM consist exclusively of 3-filaments with diameter $d(3) = 13$ nm and length $L_n = 470$ nm ($m = 27$), where L_n and m are the number-averaged length and a sharpness parameter of the length distribution, respectively. (2) They split into a mixture of 2- and 1-filaments (both with $L_n = 470$ nm and $m = 27$) on lowering ionic strength from 134 to 44 mM and vice versa. (3) The diameter of the 1-filament is $d(1) = 7.5$ nm. The size of ν is equal to the number of myosin molecules per 14.3 nm repeat mentioned above. In terms of the ν-filament, we will discuss the present observations.

MATERIALS AND METHODS

Preparation of synthetic myosin filaments

Rabbit skeletal myosin was prepared according to a conventional method (Perry, 1955). After several purification steps, the myosin preparation in a stock buffer solution (0.3 M KCl, 5 mM K_2HPO_4, 5 mM KH_2PO_4, 0.1 mM ethylenediaminetetraacetic acid (EDTA), 1 mM dithiothreitol (DTT), pH 6.7) was finally centrifuged at 120,000 × g for 3 h, and the supernatant fraction was frozen with liquid nitrogen and stored at −80°C until use. The frozen preparation of myosin molecules in the stock buffer was thawed before each set of experiments. To this myosin preparation was rapidly added a buffer solution without KCl (10 mM tris(hydroxymethyl)-aminomethane-HCl (Tris-HCl), 0.1 mM EDTA, 1 mM DTT, pH 8.3 at 10°C). By this "rapid dilution" of the KCl concentration to about 0.1 M, myosin molecules polymerized into filaments. Then the filament solution was dialyzed for 12 h against one of the buffer solutions listed in Table 1, unless otherwise stated. We call hereafter our filament preparation "EDTA-Myosin" or "Mg-Myosin" depending on the condition of dialysis. After the

Received for publication 1 September 1994 and in final form 18 October 1994.

Address reprint requests to Dr. Satoru Fujime, Graduate School of Integrated Science, Yokohama City University, 22-2 Seto, Kanazawa-ku, Yokohama 236, Japan. Tel.: 045-787-2306; Fax: 045-787-2316 (deceased on 23 December, 1994).

0006-3495/95/02/609/10 $2.00

TABLE 1 Experimental conditions

	Ionic strength (130 mM, pH 8.3, T = 10°C)	
	EDTA-myosin	Mg-myosin
KCl	120 mM	varied*
Tris-HCl	10 mM	10 mM
EDTA	0.1 mM	none
$MgCl_2$	none	1, 3, 5 mM
DTT	1 mM	1 mM

*Depending on [$MgCl_2$], [KCl] was varied so as to give the ionic strength of 130 mM.

dialysis, the preparation was centrifuged at 50,000 × g for 3 h on a swinging bucket rotor. To the supernatant was added the dialysis solution through a 25 nm membrane filter, adjusting the myosin concentration to 1 mg/ml, unless otherwise stated. When ATP (ADP) was added to the filament preparation in a scattering cell, a small volume of the concentrated ATP (ADP) solution adjusted to pH 8.3 was added to avoid a dilution of components in the scattering cell. In what follows, the brackets [...] mean the concentration of chemicals or ion species, and [ATP] (=[Mg-ATP^{2-}] + [ATP^{4-}]) and [Mg] (=[Mg-ATP^{2-}] + [Mg^{2+}]) mean concentrations of total ATP and Mg in the medium, respectively; [ATP] = [ATP^{4-}] when [Mg] = 0 and [Mg] = [Mg^{2+}] when [ATP] = 0.

DLS measurements

General background information about the DLS method is found in standard textbooks (Chu, 1974; Berne and Pecora, 1975; Schmitz, 1990). An (8 × N)-bit digital correlator (K7032C, Malvern Instruments, U.K.) was used to measure the intensity autocorrelation function of the scattered light. A 488 nm beam from an Ar^+ ion laser (Model 95, Lexel Corp., CA) was used as a light source. Our spectrometer was essentially the same as that detailed elsewhere (Fujime et al., 1984). The temperature of the sample in the scattering cell was controlled at 10 ± 0.1°C. The intensity autocorrelation function $G^2(t)$ is related to the normalized field correlation function $g^1(t)$ of the scattered light by

$$G^2(t) = B\{\beta|\, g^1(t)|^2 + 1\}, \tag{1}$$

where $t = mt_s$ ($m = 1, 2, 3, \cdots, 256$; t_s, the sampling time), B is the baseline level ($B^{1/2} = I_s$, the static scattering intensity), and β is a constant (about 0.7 in our optical setup). For a monodisperse suspension of small particles, we have a simple form of $g^1(t) = \exp(-DK^2t)$, where D is the translational diffusion coefficient of the particle and K is the length of the scattering vector, which equals $(4\pi/\lambda)\sin(\Theta/2)$ (λ, the wavelength of the light in the medium; Θ, the scattering angle). The actual form of $g^1(t)$ of our system is a sum of exponential decays because of possible contributions to the decay of $g^1(t)$ from rotational and anisotropy in translational motions and length distribution of scatterers. Then the following expansion method is used to obtain a measure of the average decay rate $\langle G\rangle$:

$$g^1(t) = (1 + m_2t^2 - m_3t^3)\exp(-\langle G\rangle t) \tag{2}$$

The quantity $\langle G\rangle/K^2$ has the same dimension as that of D (cm²/s) and is called an apparent diffusion coefficient, D_{app}.

Except for measurements of D_{app} and I_s of EDTA-myosin after addition of ATP, each point shows the average of 5–10 runs, of which error size was much less than (within) the size of symbols for D_{app} and I_s for the same (different) preparations of the filaments. For EDTA-myosin after addition of ATP, monotonous and smooth changes in D_{app} and I_s with time were obtained, assuring a reasonable accuracy of single measurement of each point. In this case, however, the extrapolated values of D_{app} and I_s to time 0 (*arrows* in Fig. 4) changed from measurement to measurement, but scatter of these extrapolated values for three independent measurements was in the size of symbols in Fig. 5 *a*).

Theoretical considerations

The apparent diffusion coefficient for a rigid rod with length L is theoretically given by

$$D_{app} = D_0 + (L^2/12)D_r f_1(k) + (D_3 - D_1)[f_2(k) - \tfrac{1}{3}], \tag{3}$$

where $D_0 = (2D_1 + D_3)/3$ is the overall translational diffusion coefficient, D_3 and D_1 are, respectively, the translational diffusion coefficients parallel and perpendicular to the long axis of the rod, D_r is the end-over-end rotational diffusion coefficient, and $f_1(k)$ and $[f_2(k) - \frac{1}{3}]$ are, respectively, the weight factors that depend on $k = KL/2$, numerical values of $f_1(k)$ and $f_2(k)$ having been tabulated (Maeda and Fujime, 1984). On the right hand side of Eq. 3, the first term is due to overall translation, the second term to rotation, and the third term to anisotropy in translation. For a smooth cylinder (rigid rod) with length L and diameter d, diffusion coefficients are given by

$$D_1 = (k_BT/4\pi\eta L)[Lp - 0.19 + 4.2(Lp^{-1} - 0.39)^2] \tag{4a}$$

$$D_3 = (k_BT/2\pi\eta L)[Lp - 1.27 + 7.4(Lp^{-1} - 0.34)^2] \tag{4b}$$

$$D_r = (3k_BT/\pi\eta L^3)[Lp - 1.45 + 7.5(Lp^{-1} - 0.27)^3], \tag{4c}$$

where k_B is the Boltzmann constant, T is the absolute temperature, η is the solvent viscosity, and $Lp = \ln(2L/d)$ (Broersma, 1969a, b). Neglecting the minor terms, the last term in each of $[\cdots]$ in Eqs 4a–c, we have $D_1 = (k_BT/4\pi\eta L)\,(Lp - 0.19)$, $(D_3 - D_1) = (k_BT/4\pi\eta L)(Lp - 2.35)$ and $(L^2/12)D_r = (k_BT/4\pi\eta L)(Lp - 1.45)$. Then, by noting $D_0 - (D_3 - D_1)/3 = D_1$, we have

$$D_{app} = (k_BT/4\pi\eta L)(A \cdot Lp - B), \tag{3'}$$

where $A = 1 + f_1(k) + f_2(k)$ and $B = 0.19 + 1.45f_1(k) + 2.35f_2(k)$. At the scattering angle of 90° and L = 680 nm (see below), we have $f_1(k) = 0.801$ and $f_2(k) = 0.0415$ from the tabulated values, or $A = 1.84$ and $B = 1.45$. In what follows, D_{app} values at 10°C are given without any correction.

Let M be the filament mass and N be the number of filaments in solution. Then, we have $MN = C_f$ (C_f: the concentration, in a proper unit, of myosin molecules incorporated into filaments, which is equal to the total myosin concentration C in solution if monomers/dimers coexisting with polymers can be ignored). The scattering intensity can be written as $I_s \propto NM^2P(K) = MC_fP(K)$, where $P(K)$ denotes the scattering function. For rods with length L and diameter d, we have M/N_A = (volume of a rod)/$v = \pi(d/2)^2L/v$ (N_A, Avogadro's number; v, specific volume). If $v \approx 0.73$ (a typical value for proteins) is assumed, the diameter d in the above equation is that of a "compact" rod (Mochizuki-Oda and Fujime, 1988). Because a myosin filament has radial projections, its diameter $\langle d\rangle$ determined from a radial mass distribution is larger than that of the compact rod. However, as far as M and L are equal, respectively, to those of the compact rod, d^2/v should be constant irrespective of the configuration of projections (if minor change in v due to possible change in conformation of protein is ignored). To express M of the filament with length L, therefore, we use a relation $M \propto d^2L$ with d of the compact rod without loss of generality. Then, we have $I_s \propto d^2LC_fP(K)$, or

$$I_s \propto d^2C_f \tag{5}$$

because $P(K) = (\pi/KL)[1 - (2/\pi)\,(1/KL)\{1 + \sin(KL)/KL\}][1 - (K\langle d\rangle/4)^2]$ for large KL and small $K\langle d\rangle$ of the present interest can be approximated as $P(K) \approx (\pi/KL)$ (note that at the scattering angle of 90°, $KL = 17$ or $(2/\pi)\,(1/KL) = 0.037$ for L = 680 nm and $(K\langle d\rangle/4)^2 = 0.06$ for $\langle d\rangle$ = 40 nm; see later for L and $\langle d\rangle$ values). Namely, an increase in d (in L) increases the I_s value strongly (very weakly) provided that C_f is very close to C. On the other hand, ignoring a minor term, B, in Eq. 3′, we have

$$D_{app} \propto \ln(2L/d)/L \tag{6}$$

an increase in L (in d) decreases the D_{app} value strongly (very weakly). In addition to this, it should be noted that D_{app} is very weakly dependent on C (or N) provided that L is constant, i.e., $D_{app} = (1 + k_DC)D_{app}(C = 0)$ with small k_D. Quite different behaviors of I_s and D_{app} against d and L (and C) are very important in this study.

In what follows, we use such terms as "thickening" and "thinning" of filaments ("lengthening" and "shortening" of filaments) instead of increase and decrease in d (in L) respectively. A comment to this is given here to avoid confusion. As far as C_f is close to C, a change in M due to changes in d and/or L alters the size of N ($=C_f/M$); thinning and thickening mean, respectively, splitting into, and association of, subfilaments mentioned in the Introduction, and lengthening and shortening require reorganization of subfilaments (dynamic equilibrium among filaments with various sizes keeping negligibly small amount of monomers/dimers). On the other hand, when C_f decreases as a result of depolymerization (dynamic equilibrium between polymers and monomers/dimers), shortening means removal of myosin molecules from both ends of (sub)filaments (no change in N), but thinning means either splitting into subfilaments (increase in N) or, although unlikely, removal of myosin molecules from surfaces of (sub)filaments (no change in N). In this case, care has to be taken in use of Eq. 5.

Polydispersity in L and d would affect the results. However, the length distribution has very little effect on the results as far as the polydispersity index m is larger than 25 (Mochizuki-Oda and Fujime, 1988), and D_{app} is very insensitive to polydispersity in d (Eq. 6). Therefore, our main point discussed below, that is, thinning without shortening up to a certain ligand concentration, is highly correct provided that d in Eq. 5 is regarded as the weight-averaged one.

Electron microscopy

The sample on a grid was washed twice with cold buffer, negatively stained with unbuffered 4% uranyl acetate, and examined on an electron microscope (JEOL 1200EX, Tokyo), operating voltage being 80 kV. The size distribution of the filaments was measured on the enlarged photographs.

RESULTS

Effect of ATP on D_{app} of EDTA-myosin at various pH values

We first studied the effect of ATP on the size of D_{app} of EDTA-myosin at various pH values. On increasing the pH value from 6.0 to 9.3, the size of D_{90} decreased to a minimal value at pH 7.5 and then increased, where D_{90} denotes D_{app} at the scattering angle of 90°. Fig. 1 shows the D_{90}(ext)/D_{90}(init) versus pH relationship for EDTA-myosin preparations, where D_{90}(init) and D_{90}(ext) denote, respectively, those before and just after the addition of ATP to a final concentration of 2 mM. (For estimation of D_{90}(ext), see later subsection.) It is clearly seen from Fig. 1 that the ratio is unity at acidic and neutral pH values, whereas it greatly increases at alkaline pH values.

Most experiments on assembly have been done on two classes of myosin filaments, those formed at pH 6.8–7.5 and those formed at 7.8–8.5 at physiological ionic strength. These classes are respectively known as pH 7 and pH 8 filaments. As a general rule, the more alkaline the medium, the shorter, thinner, and less stable the filaments (Davis, 1988). The pH 8 filaments split into subfilaments on lowering ionic strength of the medium (Mochizuki-Oda and Fujime, 1988) and are sensitive to ATP (Fig. 1; see also Harrington and Himmelfarb, 1972) and to Mg^{2+} (Figs. 2 and 3 given below; see also Persechini and Rowe, 1984; Maeda et al., 1991). In what follows, therefore, we fixed the pH value of preparations to 8.3 at 10°C.

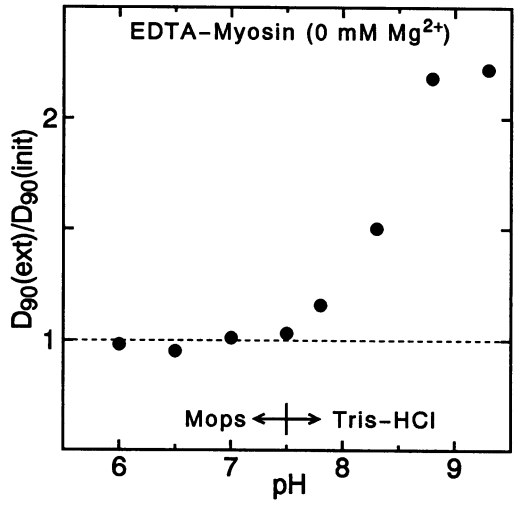

FIGURE 1 The D_{90}(ext)/D_{90}(init) vs. pH relationship for EDTA-myosin. D_{90}(init) and D_{90}(ext) denote the diffusion coefficients before and just after, respectively, the addition of 2 mM ATP. At acidic pH values, 10 mM 3-[*N*-morpholino]propanesulfonic acid (Mops) was used instead of 10 mM Tris-HCl in Table 1.

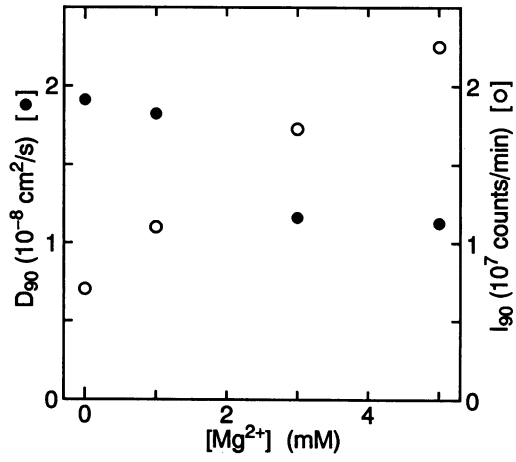

FIGURE 2 The D_{90} and I_{90} vs. [Mg^{2+}] relationships at the myosin concentration of 1 mg/ml.

The D_{90} and I_{90} vs. [Mg^{2+}] relationships

At pH 8.3 at 10°C, the D_{90} and I_{90} versus [Mg^{2+}] relationships at the myosin concentration of 1 mg/ml were obtained as shown in Fig. 2, where I_{90} denotes the scattering intensity I_s at the scattering angle of 90°. With increase in [Mg^{2+}], I_{90} increased and D_{90} decreased. (Because Fig. 2 just summarizes the average values of D_{90} and I_{90} given below for EDTA-myosin and Mg-myosin ([Mg^{2+}] = 1, 3, and 5 mM) in the absence of ATP/ADP, the observed points are so coarsely spaced that it is rather difficult to determine [Mg^{2+}] for which the midpoints of changes in D_{90} and I_{90} appear.)

Referring to Eqs. 5 and 6, the data in Fig. 2 qualitatively suggest that the large decrease in D_{90} and increase in I_{90} in a [Mg^{2+}] range from 0 to 3 mM are due to lengthening and thickening of the filaments, whereas very little decrease in

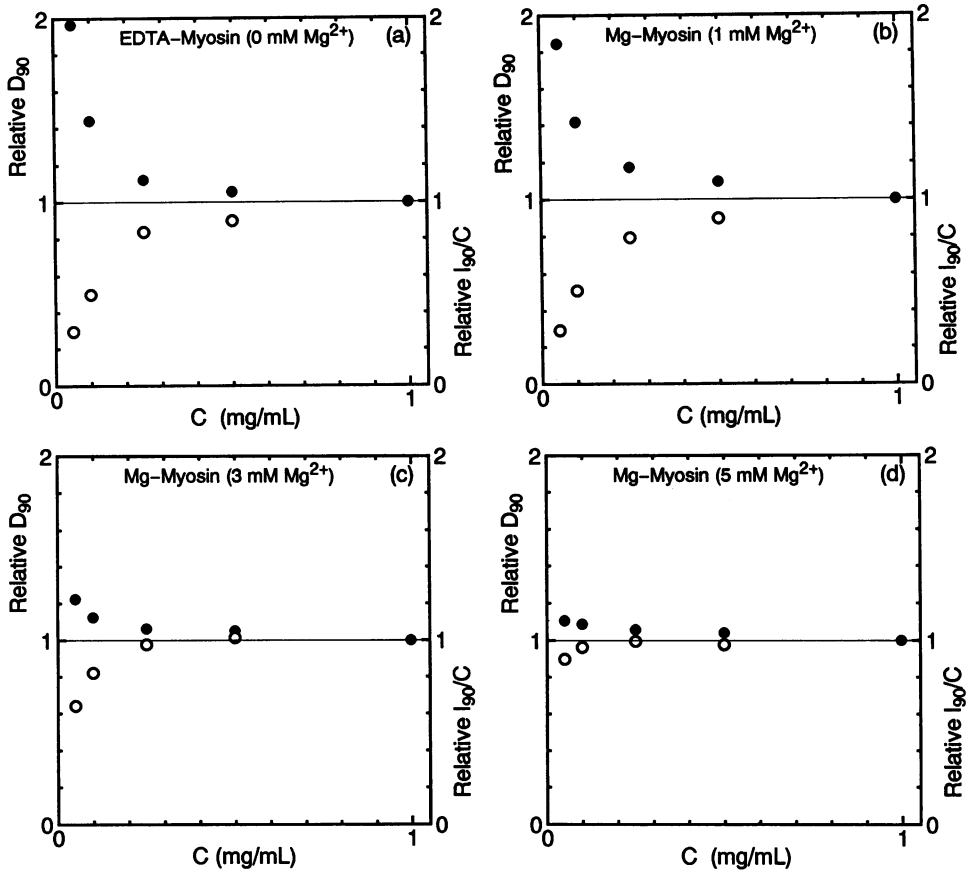

FIGURE 3 The D_{90} and I_{90}/C vs. C relationships. Both D_{90} and I_{90}/C are normalized to unity at C = 1 mg/ml, where C is the myosin concentration. [Mg^{2+}] in the medium are 0 mM (*a*), 1 mM (*b*), 3 mM (*c*), and 5 mM (*d*).

D_{90} and a substantial increase in I_{90} in a range from 3 to 5 mM are due mostly to thickening of the filaments. The molecular mass is proportional to (s/D_0), where s is the sedimentation velocity (Mochizuki-Oda and Fujime, 1988). We did not measure the s values of our own preparations. If, however, a sigmoidal increase of s against log[Mg^{2+}] (a midpoint of this change is at 1.5 mM) is assumed (Persechini and Rowe, 1984), the molecular mass would largely increase with [Mg^{2+}] because of increase in s and decrease in D_0 ($=D_{app}$ at the limit of zero scattering angle) with [Mg^{2+}].

The D_{90} and I_{90} vs. C relationships

To see an effect of Mg^{2+} ions on the stability of myosin filaments, the C-dependence of D_{90} and I_{90}/C (C: myosin concentration) was studied (Fig. 3 *a–d*). In Fig. 3, both "Relative D_{90}" and "Relative I_{90}/C" are normalized to unity at C = 1 mg/ml. Deviations from unity of both relative D_{90} and I_{90}/C become large as C decreases; the higher the [Mg^{2+}], the smaller the deviations. The binding of Mg^{2+} to the low affinity sites of a myosin filament (filament core) stabilizes the filament structure.

Effects of added [ATP] and [ADP] on D_{90} and I_{90} of EDTA-myosin

Fig. 4 shows the dependences on [ATP] of D_{90} (*a*) and I_{90} (*b*). Here and hereafter, I_{90} was normalized by that before addition of ATP (or ADP). After ATP addition, D_{90} (I_{90}) immediately increased (decreased) to a certain level dependent on the concentration of added ATP ([ATP]), and then gradually decreased (increased) with time during the hydrolytic reaction. The rate of changes in D_{90} and I_{90} approximated the rate of ATP hydrolysis, suggesting that the recovery in D_{90} and I_{90} with time was due to the depletion of ATP (about 1 mM ATP would be hydrolyzed for every 1400 s (23 min) under the present condition). For higher [ATP], however, recovery in D_{90} and I_{90} with time was not observed, suggesting that the elevation of the reaction products, ADP and inorganic phosphate, could also act to increase D_{90} and decrease I_{90} as ATP did. Then, the measurements similar to the above ones were made with ADP. After ADP addition, D_{90} (I_{90}) immediately increased (decreased) to a certain level dependent on [ADP], but no appreciable recovery in D_{90} and I_{90} with time was observed, as expected.

Because we could not measure both D_{90} and I_{90} immediately after the addition of ATP, we estimated D_{90}(ext) and I_{90}(ext) by extrapolating the observed values to time 0 (see arrows in Fig. 4, *a* and *b*). Omitting "ext," D_{90} and I_{90} thus estimated are shown against [ATP] in Fig. 5 *a* and against [ADP] in Fig. 5 *b*. The binding of ligands (ATP and ADP) to a myosin filament (filament core; Harrington and Himmelfarb, 1972) destabilizes the filament structure, which is in contrast to the binding of Mg^{2+}. The I_{90} vs. [ATP] and [ADP] relationships are virtually the same as the earlier results by turbidimetry (Harrington and Himmelfarb, 1972).

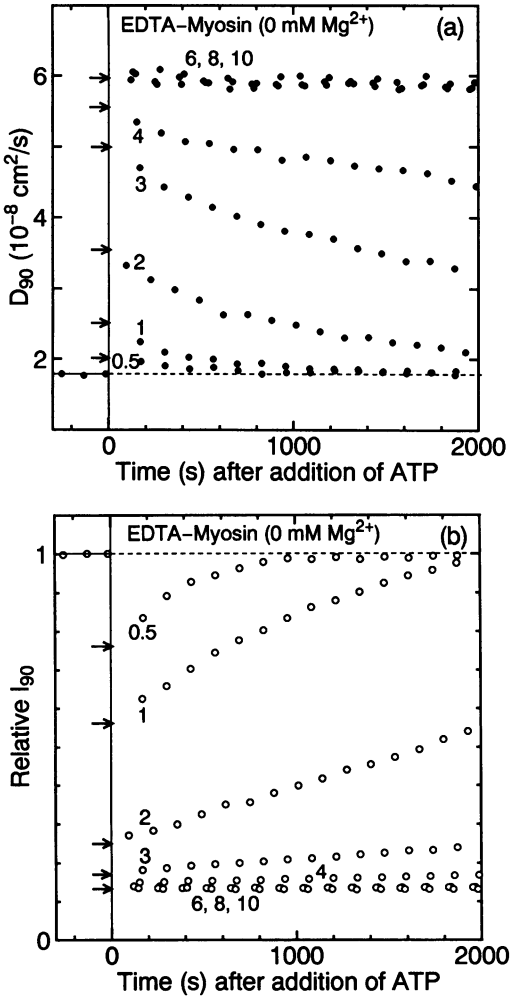

FIGURE 4 The time-dependent changes in D_{90} (*a*) and I_{90} (*b*) for EDTA-myosin after addition of ATP. Added [ATP] are indicated in the figure (in mM units). The arrows indicate the extrapolated values of D_{90} and I_{90} to time 0. Here and hereafter, I_{90} is normalized by that before the addition of ATP (ADP).

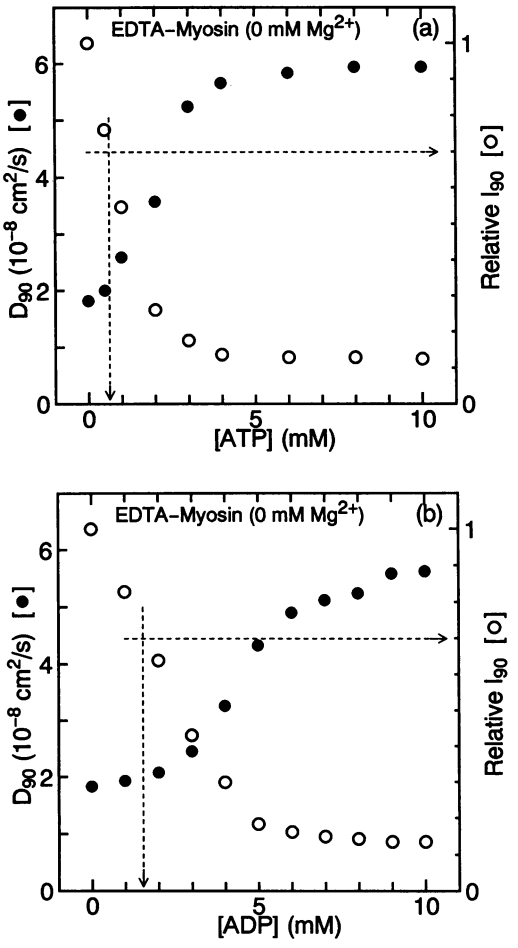

FIGURE 5 The D_{90} and I_{90} vs. [ligand] relationships for EDTA-myosin at 1 mg/ml protein. (*a*) Ligand is ATP, and both D_{90} and I_{90} are those extrapolated to time 0 (see *arrows* in Fig. 4). (*b*) Ligand is ADP. Dashed arrows indicate [ligand] where $I_{90} = 0.7$.

Our results show that (1) up to ligand concentrations where I_{90} decreases by 20–30%, D_{90} increases very little (see *dashed arrows* in Fig. 5, *a* and *b*), and (2) the limiting value of $D_{90} \approx 6 \cdot 10^{-8}$ cm^2/s is close to the diffusion coefficient of a myosin dimer, $6.5 \cdot 10^{-8}$ cm^2/s at 10°C (Herbert and Carlson, 1971). The item (1) suggests thinning of myosin filaments, or splitting into subfilaments. The item (2) suggests that the depolymerization is almost complete at 10 mM [ATP] or [ADP].

Effects of added [ATP] on D_{90} and I_{90} of Mg-myosin

The measurements similar to the above were made for Mg-myosin. In this case, the rate of Mg-ATP hydrolysis was so low that the DLS measurements were relatively easy. The left panels of Fig. 6 show the D_{90} and I_{90} vs. [ATP] relationships for Mg-myosin at [Mg] = 1 mM (*a*), 3 mM (*b*), and 5 mM (*c*). These results clearly show that (1) there are two competing effects: one is the stabilizing effect of free-Mg^{2+}, and the other is the destabilizing effect of free-ATP, and (2) at lower concentrations of [ATP] D_{90} stays constant whereas I_{90} greatly decreases (this is most clearly seen at [Mg] = 5 mM).

The D_{90} value does not increase appreciably in a range of [ATP] from 0 to a certain value where I_{90} drops by 30% (see *dashed arrows* in the left panels of Fig. 6). In such a range, the filament length might keep its original value, whereas the average diameter would decrease (cf. Eqs. 5 and 6). In fact, we can estimate the average diameter $d = 0.84d_0$ from a relation $I_{90}/I_{90}([ATP] = 0\ mM) = 0.7 = (d/d_0)^2$ (if C_f unchanged, see Eq. 5). Then, from a relation $\ln(2L_0/d) = \ln(2L_0/d_0) + \ln(d_0/d) = 4.44 + 0.17 = 4.61$ for $L_0 = 680$ nm and $d_0 = 16$ nm at [ATP] = 0 mM (and [Mg] = 3 mM; see later), we can estimate $D_{90}/D_{90}([ATP] = 0\ mM) = 4.61/4.44 = 1.04$ from Eq. 6, or more precisely, $= (4.61A - B)/(4.44A - B) = 1.05$ from Eq. 3′. Namely, a decrease in I_{90} by 30% corresponds to filament thinning by 16% with no shortening, and this thinning results in an increase in D_{90} by only 4–5%. Outside the above range of [ATP], D_{90} increases substantially, so that not only thinning but also shortening (depolymerization) of filaments should occur with increase in [ATP].

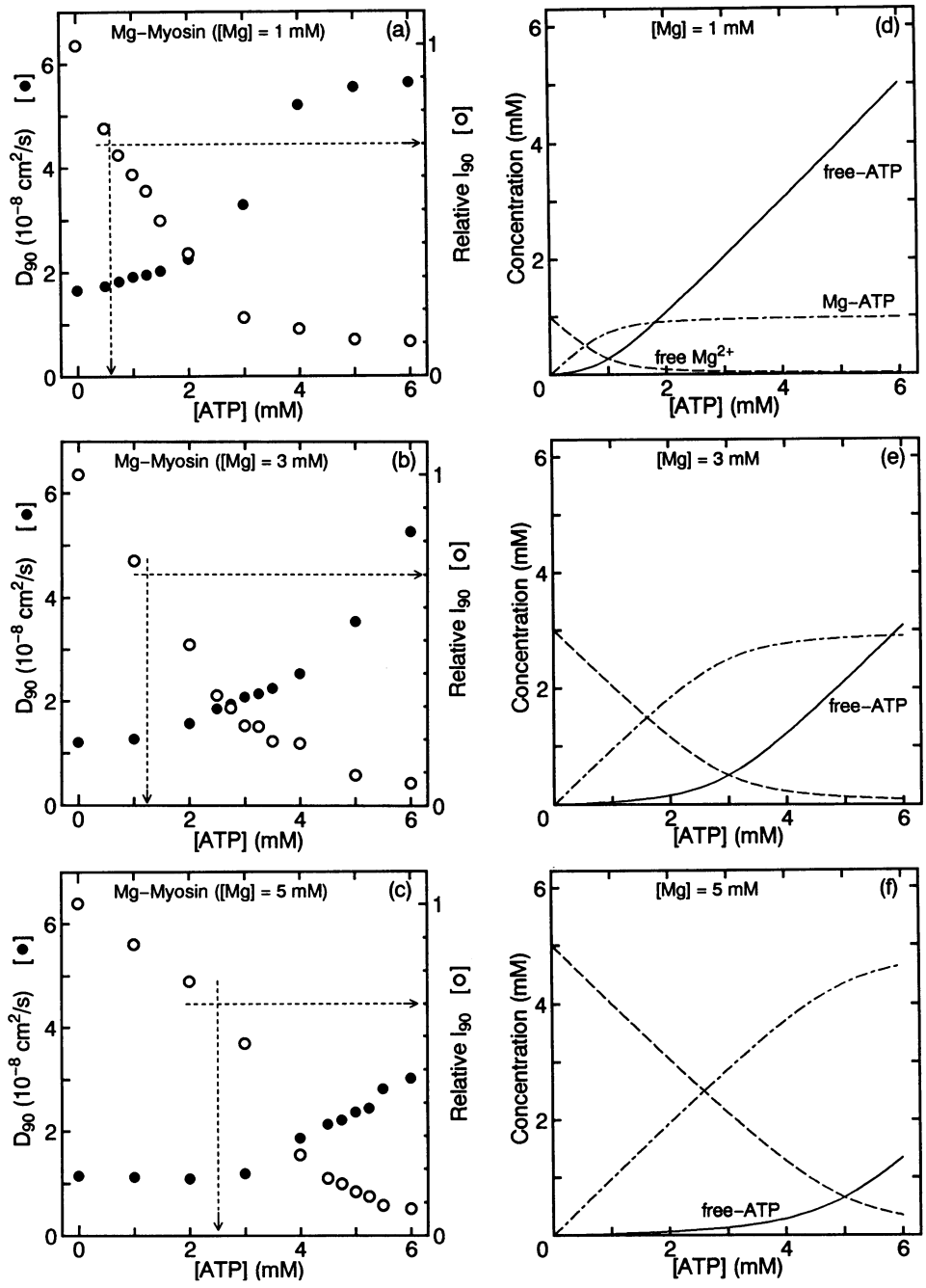

FIGURE 6 The D_{90} and I_{90} vs. [ATP] relationships for Mg-myosin at 1 mg/ml protein (*left panels*), and the [ATP^{4-}], [Mg^{2+}], and [Mg-ATP^{2-}] vs. [ATP] relationships (*right panels*). [Mg] = 1 mM (*a*, *d*), 3 mM (*b*, *e*) and 5 mM (*c*, *f*). Dashed arrows in left panels indicate [ATP] where I_{90} = 0.7.

For later discussion, the concentrations of free-ATP ([ATP^{4-}]), free-Mg^{2+} ([Mg^{2+}]), and Mg-ATP ([Mg-ATP^{2-}]) are computed for the association constant of K_a(Mg/ATP) = $10^{3.89}$ M^{-1} at pH 8.3 and 10°C (Khan and Martell, 1962). Because the myosin concentration, 2 μM for C = 1 mg/ml, is three orders of magnitude lower than [Mg] and [ATP] of 1–5 mM, Mg^{2+} and ATP^{4-} bound to myosin molecules can be ignored. Then, solving

$$K_a(\text{Mg/ATP}) = [\text{Mg-ATP}^{2-}]/[\text{Mg}^{2+}][\text{ATP}^{4-}] \quad (7)$$

for given values of [Mg] (= [Mg^{2+}] + [Mg-ATP^{2-}]) and [ATP] (= [ATP^{4-}] + [Mg-ATP^{2-}]), we have the results shown in the right panels of Fig. 6 for [Mg] = 1 mM (*d*), 3 mM (*e*), and 5 mM (*f*).

From the data in Figs. 2, 3, 5, and 6, we can construct Fig. 7, which shows the effect of equimolar [Mg/ATP] on D_{90} and I_{90} of "EDTA-Myosin," where equimolar [Mg/ATP] means [Mg] = [ATP]. The numbers on the upper x axis in Fig. 7 show the concentrations of free-ATP ([ATP^{4-}] = [Mg^{2+}]; cf. right panels in Fig. 6) in the medium. When we read Fig. 7 as the D_{90} and I_{90} vs. [ATP^{4-}] relationships for EDTA-myosin, then we find quite a good correspondence with those at first three points (0, 0.5, and 1 mM ATP) in Fig. 5 *a*.

The D_{app} vs. K^2 relationship of Mg-myosin

Until now, we showed only the D_{90} (and I_{90}) at various conditions. To complete our DLS study, some of the D_{app} vs. K^2

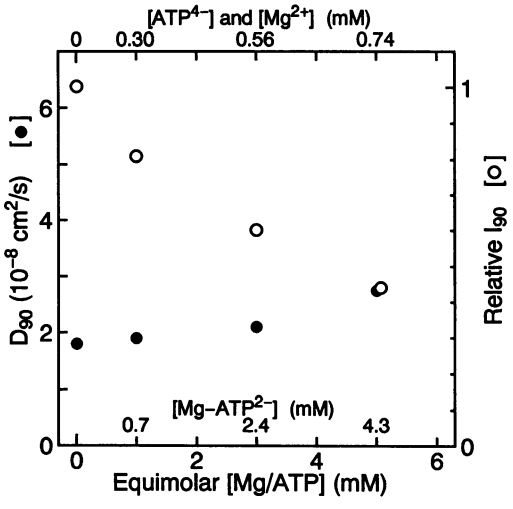

FIGURE 7 The D_{90} and I_{90} vs. equimolar [Mg/ATP] relationships at the myosin concentration of 1 mg/ml. The upper x axis shows $[ATP^{4-}]$ $(=[Mg^{2+}])$, and numbers inside the frame show $[Mg\text{-}ATP^{2-}]$. This figure was constructed from data in Figs. 3 *a*, 5, *a* and *b*, and 6 *a–c*, where I_{90} was renormalized with reference to data in Fig. 2.

relationships are shown in Fig. 8 that were measured over the scattering angles from 30° to 130° for 1 mg/ml Mg-myosin ([Mg] = 3 mM) at [ATP] = 0, 1, and 3 mM. A theoretical simulation (curves in the figure) of the D_{app} vs. K^2 relationships is given later.

The size distribution of filaments

On electron micrographs of synthetic myosin filaments, we counted the number $N(L_j)$ of filaments with lengths in a range $(L_j, L_j + \delta)$. The number-average length L_n was determined by $L_n = \Sigma_j L_j N(L_j)/\Sigma_j N(L_j)$. The length distribution $N(z)$ was then normalized to unity at z $(=L/L_n)$ = 1. The results for Mg-myosin at [Mg] = 3 mM are shown in Fig. 9; [ATP] = 0 mM (*a*), 2.5 mM (*b*), and 5 mM (*c*). The observed distributions were fitted to the Schultz-Zimm distribution function $S(z) = C_m z^m \exp[-(m+1)z]$, or $N(z) = S(z)/S(1)$, where C_m is the normalization constant and m is the parameter determining the sharpness of the distribution; the larger the m value, the sharper the distribution. The fitted curves are also shown in Fig. 9 with solid lines. For filaments at [Mg]= 3 mM, L_n (m) are 680 nm (26), 470 nm (16), and 300 nm (10) for [ATP] = 0, 2.5, and 5 mM, respectively.

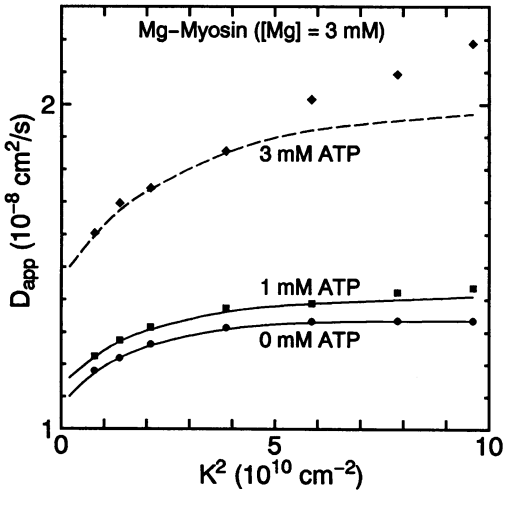

FIGURE 8 The D_{app} vs. K^2 relationships for Mg-myosin at 1 mg/ml. [Mg] = 3 mM, and [ATP] = 0, 1, and 3 mM from bottom to top. See the text for evaluation of the theoretical curves (—— and – – – –).

It was very difficult to determine the average diameter from images of negatively stained filaments. The major fraction of filaments gave the diameter d^i = 18–19 nm at the bare zone, where the superscript "i" denotes "from images." In our previous study (Mochizuki-Oda and Fujime, 1988), we obtained d^i/d^s = (15 nm)/(13 nm) and ν = 3 for Mg-myosin at [Mg] = 1 mM, where the superscript "s" denotes "from sedimentation." As a rough estimate of the diameter, we then take $d\,[=d^s]$ = (18–19 nm)/(15/13) = 16 nm for the present Mg-myosin at [Mg] = 3 mM and [ATP] = 0 mM. (This kind of conversion is not necessarily required in our discussion if the diameter $d(1)$ $[=d^s(1)]$ = 7.5 nm of 1-filaments is replaced with $d(1)$ $[=d^i(1)] = d^i/\nu^{1/2}$ = 8.7 nm for d^i = 15 nm and ν = 3. See the last paragraph of Introduction. For more details about d^s and $d^s(\nu)$, see our previous study.) On our micrographs, it was unable to distinguish 13 nm filaments from 16 nm filaments (cf. d/d_0 = 0.84 described in a previous subsection). However, we observed images of distinctly thinner (than 16 nm) filaments presumably corresponding to single subfilaments (1-filaments), and their number relative to that of 16 nm filaments increased at [ATP] = 2.5 mM.

DISCUSSION

Effect of Mg^{2+}

Because the diameter of our Mg-myosin at [Mg] = 3 mM is determined to be 16 nm (from electron microscopy), we can estimate the number of subfilaments to be $\nu = (16/7.5)^2$ = 4.6, suggesting a mixture of 3- and 6-filaments. Because $D_{90} = 1.8 \cdot 10^{-8}$ cm²/s of our Mg-myosin at [Mg] = 1 mM is very close to that of our earlier result, we assume that our Mg-myosin at [Mg] = 1 mM has length 470 nm and diameter 13 nm as in Mochizuki-Oda and Fujime (1988). If we assume the same value for C_f at [Mg] = 1 and 3 mM, we can then estimate I_{90}([Mg] = 3 mM)/I_{90}([Mg] = 1 mM) = $(16/13)^2$ = 1.5 from Eq. 5, and D_{90}([Mg] = 3 mM)/D_{90}([Mg] = 1 mM) = [ln(2 · 680/16)/680]/[ln(2 · 470/13)/470] = 0.72 from Eq. 6. These estimates, 1.5 and 0.72, are found to be in a reasonable agreement, respectively, with the observed ratios 1.7 and 0.68 for I_{90} and D_{90} at [Mg] = 3 and 1 mM in Fig. 2.

The above analysis suggests that the molecular mass of myosin filaments increases 2.2 times in association with lengthening by 680/470 1.5 times and thickening by 16/13 1.2 times when [Mg] is raised from 1 to 3 mM. A slight but definite decrease in D_{90} and substantial increase in I_{90} in a [Mg] range from 0 to 1 mM are due to a little lengthening and thickening of the filaments. On the other hand, a sub-

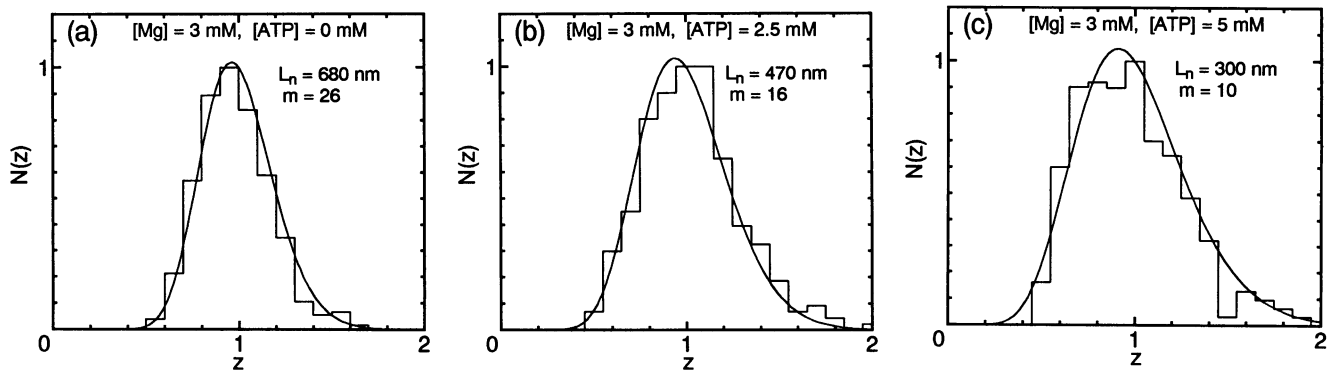

FIGURE 9 The $N(z)$ vs. z relationships for Mg-myosin. The number $N(z)$ is normalized to unity at $z = 1$, where $z = L/L_n$ (L_n being the number-averaged length). [Mg] = 3 mM, and [ATP] = 0 mM (*a*), 2.5 mM (*b*), and 5 mM (*c*). The solid curves show the least-squares fitted ones to the Schultz-Zimm function (see the text).

stantial increase (26%) in I_{90} and very little decrease (−4%) in D_{90} in a [Mg] range from 3 to 5 mM are mostly due to thickening of the filaments. In fact, a change in ν from $(16/7.5)^2 = 4.6$ at [Mg] = 3 mM to $(18/7.5)^2 = 5.8$ at [Mg] = 5 mM results in an increase in I_{90} of $(18/16)^2 = 1.27$ (+27%) and an decrease in D_{90} of $\ln(2 \cdot 680/16)/\ln(2 \cdot 680/18) = 0.97$ (−3%). These estimates can account for the changes in I_{90} and D_{90} with an increase in [Mg] from 3 to 5 mM (Fig. 2).

Let C_c ($=C - C_f$) be the critical concentration of monomers/dimers coexisting with polymers (filaments). If $C_f \gg C_c$ even at $C = 0.05$ mg/ml (the lowest concentration in Fig. 3), we can ignore the depolymerization of filaments to keep C_c constant on lowering C. Putting $C_f/C = C_{f0}/C_0 = 1$, we have (Relative I_{90}/C) $= (d/d_0)^2$ from Eq. 5, and (Relative D_{90}) $= [\ln(2L_0/d)/\ln(2L_0/d_0)]$ from Eq. 6, where quantities with suffix 0 denote those at $C = 1$ mg/ml. If splitting into subfilaments is assumed to occur with decrease in C, (Relative I_{90}/C) = 1/3 at $C = 0.05$ mg/ml gives $(d/d_0) = 0.58$. This d ($=0.58d_0 = 7.5$ nm $= d(1)$) gives (Relative D_{app}) = 1.12 for $L_0 = 470$ nm and $d_0 = 13$ nm. This size of 1.12 (+12%) does not account for the observed values of about 1.9 at 0 and 1 mM Mg^{2+} in Fig. 3, *a* and *b*.

The above analysis suggests that C_f is not much greater than C_c at low C, and shortening (depolymerization) of filaments cannot be ignored to keep C_c constant on lowering C. In such a situation, contributions to D_{app} and I_s from monomers/dimers cannot be ignored, and we have

$$D_{app} = [D_{app}(m)I_s(m) + D_{app}(p)I_s(p)]/I_s, \qquad (8)$$

where $I_s = I_s(m) + I_s(p)$, $I_s(p)$ is given by Eq. 5 and $D_{app}(p)$ by Eq. 6, and (m) and (p) denote monomer/dimer and polymer, respectively. Equation 8 states that D_{90} has a certain value in the range $[D_{90}(p), D_{90}(m)]$ depending on the ratio $I_{90}(m)/I_{90}(p)$ or C_c/C_f. Although a quantitative analysis is difficult, data in Fig. 3 suggest that the critical concentration C_c decreases with increase in $[Mg^{2+}]$.

In a range of C where (Relative I_{90}/C) is unity within experimental errors in Fig. 3, *c* and *d*, neither thinning nor shortening of filaments is expected. A slight change in D_{90} in that range of C can therefore be expressed by $D_{90}(C) = (1 + k_D C)D_{90}(C = 0)$ with $k_D \approx -0.091$ ml/mg. This k_D is a little bit smaller than that available in literature; $k_D \approx -0.13$ ml/mg for myosin minifilaments (roughly estimated from Fig. 4 in Reisler et al., 1980).

Effect of ATP and ADP on EDTA-myosin

At [ATP] = 0.5 mM in Fig. 5 *a*, we find a decrease in I_{90} by more than 20% but an increase in D_{90} by 10% at most. This suggests that thinning of the filaments occurs before shortening as $[ATP^{4-}]$ increases from 0 mM, although no measurements of D_{90} at [ATP] < 0.5 mM were made because of technical difficulties. In the case of ADP, on the other hand, thinning of the filaments before shortening is clearly seen at [ADP] < 2 mM (Fig. 5 *b*).

Thinning without shortening (no change in C_f) results in a decrease in $I_{90}(p)$ in Eq. 8 without change in $I_{90}(m)$. If $I_{90}(m)$ is not negligibly smaller than $I_{90}(p)$, Eq. 8 states that D_{90} will become more or less larger than $D_{90}(p)$ expected from Eq. 6 for pure thinning. That is, an increase in D_{90} by about 10% at 0.5 mM ATP in Fig. 5 *a* may not necessarily mean the shortening of filaments. This may also be true for the effects of ADP on EDTA-myosin in Fig. 5 *b* and of ATP on Mg-myosin at [Mg] = 1 mM in Fig. 6 *a*, because C_c is relatively high at [Mg] = 0 and 1 mM as discussed in the preceding subsection.

Another point to be noted here is that the recovery in D_{90} is faster than that in I_{90} for added [ATP] of 1 and 2 mM, for example, in Fig. 4, *a* and *b*. This may suggest that with decrease in C_c with depletion of ATP, lengthening of subfilaments occurs before their association (thickening).

Effect of ATP on Mg-myosin

As mentioned before, thinning of the filaments (splitting into subfilaments) exclusively occurs up to a certain [ATP] as indicated by a vertical arrow in each of the left panels of Fig. 6. At [ATP] higher than that, both thinning and shortening of filaments simultaneously occur with increase in C_c, the concentration of monomers/dimers.

At [Mg] = 1 mM. When [ATP] is raised, [Mg^{2+}] decreases and [ATP^{4-}] increases very rapidly (Fig. 6 *d*). Therefore, both thinning and shortening might occur from low [ATP]. Nevertheless, the increase in D_{90} is very gradual up to [ATP] = 2 mM (Fig. 6 *a*). Except this region, the D_{90} vs. [ATP^{4-}] relationship in Fig. 6 *a* is very close to the D_{90} vs. [ATP] relationship in Fig. 5 *a*.

At [Mg] = 3 mM. When [ATP] is raised from 0 to 2.2 mM, for example, [Mg^{2+}] decreases from 3 to 1 mM (Fig. 6 *e*). In this [Mg^{2+}] range, both thinning and shortening of filaments simultaneously occur, because D_{90} as well as I_{90} greatly change even in the absence of ATP (Fig. 2). Therefore, even semiqualitative interpretation of the results is not easy. However, very slight increase in D_{90} at low [ATP] is due only to thinning of filaments as [Mg^{2+}] decreases (Fig. 6 *b*). At [ATP] > 3 mM where [Mg^{2+}] < 1 mM, the size of D_{90} of Mg-myosin is the same as that of EDTA-myosin (Fig. 5 *a*) if they are compared at the same [ATP^{4-}].

At [Mg] = 5 mM. On addition of 2.5 mM ATP, [Mg^{2+}] decreases from 5 to 2.6 mM, [ATP^{4-}] increases from 0 to 0.12 mM, and [Mg-ATP] increases from 0 to 2.4 mM (Fig. 6 *f*). This decrease in [Mg^{2+}] from 5 to 2.6 mM (on addition of 2.5 mM ATP) results in the decrease in I_{90} by 30% and very little increase in D_{90} (Fig. 6 *c*). The sizes of these changes in I_{90} and D_{90} are almost exactly equal to the sizes of the decrease in I_{90} by 30% and very little increase in D_{90} when [Mg^{2+}] is lowered from 5 to 2.6 mM in the absence of ATP (Fig. 2). This suggests that only a large decrease in [Mg^{2+}] (and possibly the presence of a small amount of ATP^{4-}) induces thinning of the filaments, and a large amount of Mg-ATP^{2-} has little effect on myosin filaments (see also Fig. 7). At [ATP] higher than 2.5 mM, further decrease in [Mg^{2+}] and increase in [ATP^{4-}] induce not only thinning but also shortening (depolymerization) of filaments.

Analysis of the D_{app} vs. K^2 relationships

We assume that the myosin filament is a rigid rod, and the length distribution of our synthetic myosin filaments is given by Fig. 9 *a* for [Mg] = 3 mM and [ATP] = 0 and 1 mM. Then only the d value is left as an adjustable parameter in Eqs. 3 and 4. The average over $N(z)$ of $D_{app}(z)$ is given by $\langle D_{app}\rangle = \Sigma_j D_{app}(z_j) z_j^2 N(z_j)/\Sigma_j z_j^2 N(z_j)$ (an algorithm of this computation is found in Fujime and Kubota, 1985). The numerical results for the $\langle D_{app}\rangle$ vs. K^2 relationships for [ATP] = 0 and 1 mM are shown by solid curves in Fig. 8, where the best-fit "hydrodynamic" diameters (d^h) of the myosin filament are 85 and 75 nm for [ATP] = 0 and 1 mM, respectively. These hydrodynamic diameters are too much larger than 18–13 nm discussed above. This comes from an *extra* friction due to myosin heads radially projecting from the shaft of the filament, as detailed previously (Mochizuki-Oda and Fujime, 1988; see also the next subsection). Here we just note that the ratio of these hydrodynamic diameters, $d^h/d_0^h = 75/85 = 0.88$, can again account for the decrease in I_{90} by 22–23% (cf. $(0.88)^2 = 0.78$) and the increase in D_{90} by 4–5% in Fig. 6 *b*. The overall fitting of the D_{app} vs. K^2 relationships again suggests thinning of the filament.

An analysis of the D_{app} vs. K^2 relationship at [ATP] = 3 mM is not easy, because there are many monomers/dimers coexisting with polymers. If we tentatively assume that the solution consists only of monodisperse filaments with length 470 nm, we have the result shown by the dashed line in Fig. 8 for the hydrodynamic diameter of 70 nm. Large deviations of observed points from the dashed line at high K is not due to the flexing motions of filaments but possibly due to the fact that the K dependence is stronger in $I_s(p)$ than in $I_s(m)$ in Eq. 8. The values of d^h = 85, 75, and 70 nm correspond, respectively, to d_0 = 16, d = 14, and 13 nm, or the ν values of 4.6, 3.5, and 3.

Some remarks

Possible effects of the radial projections (cross-bridges) of the myosin filament have not been explicitly considered in our interpretation of the experimental results. Some pieces of evidence for this are listed below.

The radial projections are responsible for a very large size of the hydrodynamic diameter of the filament, d^h = 75–85 nm. As detailed previously (Mochizuki-Oda and Fujime, 1988), however, the D_{app} vs. K^2 relationship of myosin filaments can be simulated with $d = d^s$ provided that η in Eq. 4 is replaced with $\eta^* = (1.8 - 2)\eta$. The present results for [ATP] = 0 and 1 mM in Fig. 8 are also equally simulated for d = 16 and 14 nm, respectively, if we put $\eta^* = 1.9\eta$. Based on this fact, Eq. 6 with $d\,(=d^s)$ instead of d^h has been used in estimation of the ratio of D_{90} values at different conditions.

The presence of radial projections makes it plausible that the diameter $\langle d\rangle$ of the filament in the expression of $P(K) = (\pi/KL)[1 - (K\langle d\rangle/4)^2]$ (see the lines next to Eq. 5) should also be much larger than $d\,(=d^s) = 16$ nm. In fact, the slope of the KI_s vs. K^2 relationship at large K^2 gives a $\langle d\rangle$ value close to $d^h/2$ (Suzuki and Wada, 1981). Our I_s values (the results associated with those at [ATP] = 0 and 1 mM in Fig. 8) also gave a $\langle d\rangle$ value close to $d^h/2$, i.e., about 40 nm). Even for $\langle d\rangle$ = 40 nm, we have $(K\langle d\rangle/4)^2 = 0.06$ at the scattering angle of 90°. This correction term is still small, and its neglect in Eq. 5 will produce a negligibly small error, much less than 3%, in estimation of the ratio of d/d_0 at different conditions.

The ligand binding may increase the flexibility of the HMM/LMM hinge. If this were the case, an increase in the amplitude of thermal (and, if present, ATP-energized) swing of cross-bridges would result in a decrease in I_s (Fujime and Kubota, 1984). The swing amplitude may also affect the size of the extra friction arising from projections, and hence, the size of the diffusion coefficient, of the filament. However, this effect is not appreciable in our preparations, because D_{90} stays constant up to a ligand concentration where I_{90} drops by 30% of the initial.

The cross-bridges may exist in one of two possible configurations, one close to the filament axis (heads-down), and the other displaced to a distant radial position (heads-up). This two-state model has been proposed to account for the

decreased rate at which S-1 subunits are chemically cross-linked to the filament surface in a heads-up state at pH > 7.4 (Ueno and Harrington, 1981), and for sigmoidal increases in the sedimentation velocity and turbidity with the transition from heads-up to heads-down with log[Mg^{2+}] at pH 7.6 (Persechini and Rowe, 1984). It is important to distinguish changes in $\langle d \rangle$ and d^h due to a transition from heads-up to heads-down without change in M (molecular mass) from those due to splitting into subfilaments with change in M. The former changes are expected to *increase* I_{90} (but only by 10% at most; for example, changes in $(K\langle d \rangle/4)^2$ from 0.1 to 0.01), whereas the latter changes *decrease* I_{90} (Eq. 5). Furthermore, the former changes should also decrease the extra friction, and hence increase D_{90}, of the filaments. This, however, is not the case (Fig. 2). We infer that cross-bridges are always in a heads-up state in our preparations at pH 8.3.

SUMMARY

We have studied the effects of ligands on the apparent diffusion coefficient D_{app} (mostly D_{90}) and static scattering intensity I_{90} of synthetic myosin filaments at pH 8.3. By comparing the different behaviors of D_{90} and I_{90} against [Mg] and/or [ATP], we conclude that Mg^{2+} (ATP^{4-}) ions induce thickening and lengthening (thinning and shortening) of the filament. For given [Mg], an increase in [ATP] decreases [Mg^{2+}], which induces thinning of filaments as far as [ATP^{4-}] is very low, say lower than 0.1–0.2 mM, and further increase in [ATP] progressively raises [ATP^{4-}], which induces depolymerization of the filaments (cf. each pair of left and right panels in Fig. 6). Even in the case of [Mg] = 0 mM, ATP^{4-} (<0.5 mM) or ADP^{3-} (<2 mM) induces thinning of filaments without shortening (Fig. 5). There might be specific interactions of charged ligands with myosin filaments in such a way as to modify attractive and repulsive domains between subfilaments, for example, in a model of Davis (1986).

The very initial stage of this study was carried out by T. Ohtsu (one of our undergraduate students, now at Matsushita Denso Co., Tokyo). This paper is based on the master thesis of S. Takayama (now at TDK Corporation, Tokyo). We thank Dr. S. Ishiwata of Waseda University and Dr. H. Higuchi of Jikei University School of Medicine for their valuable advices to this study.

REFERENCES

Berne, B., and R. Pecora. 1975. Dynamic Light Scattering. Interscience, New York. 376 pp.

Broersma, S. J. 1969a. Rotational diffusion constant of a cylindrical particle. *J. Chem. Phys.* 32:1626–1631.

Broersma, S. J. 1969b. Viscous force constant for a closed cylinder. *J. Chem. Phys.* 32:1632–1635.

Chu, B. 1974. Laser Light Scattering. Academic Press, New York. 317 pp.

Davis, J. S. 1986. A model for length-regulation in thick filaments of vertebrate skeletal myosin. *Biophys. J.* 50:417–422.

Davis, J. S. 1988. Assembly process in vertebrate skeletal thick filament formation. *Annu. Rev. Biophys. Chem.* 17:217–239.

Fujime, S., S. Ishiwata, and T. Maeda. 1984. Dynamic light scattering study of muscle F-actin. *Biophys. Chem.* 20:1–20.

Fujime, S., and K. Kubota. 1984. Effect of cross-bridge motion on the spectrum of light quasielastically scattered from *limulus* thick myofilament suspensions. *Macromolecules.* 17:441–445.

Fujime, S., and K. Kubota. 1985. Dynamic light scattering from dilute suspension of thin discs and thin rods as limiting forms of cylinder, ellipsoid and ellipsoidal shell of revolution. *Biophys. Chem.* 23:1–13.

Harrington, W. F., and S. Himmelfarb. 1972. Effect of adenosine di-and triphosphates on the stability of synthetic myosin filaments. *Biochemistry.* 11:2945–2952.

Herbert, T. J., and F. D. Carlson. 1971. Spectroscopic study of the self-association of myosin. *Biopolymers.* 10:2231–2252.

Khan, M. M. T., and A. E. Martell. 1962. Metal chelates of adenosine triphosphate. *J. Phys. Chem.* 66:10–15.

Maeda, T., and S. Fujime. 1984. Spectrum of light quasielastically scattered from solutions of very long rods at dilute and semidilute regimes. *Macromolecules.* 17:1157–1167.

Maeda, T., M. Yamamoto, and M. Takasaki-Ohsita. 1991. Effect of Mg^{2+} on the flexural rigidity of synthetic myosin filaments. The 29th Annual Meeting of Biophysical Society of Japan, Book of Abstracts S119.

Maw, M. C., and A. J. Rowe. 1980. Fraying of A-filaments into three subfilaments. *Nature.* 286:412–414.

Mochizuki-Oda, N., and S. Fujime. 1988. Dynamic light-scattering study of synthetic myosin filaments. *Biopolymers.* 27:1389–1401.

Perry, S. V. 1955. Myosin adenosinetriphosphatase. *Methods Enzymol.* 2:582–588.

Persechini, A., and A. J. Rowe. 1984. Modulation of myosin filament conformation by physiological levels of divalent cation. *J. Mol. Biol.* 172:23–39.

Reisler, E., C. Smith, and G. Seegan. 1980. Myosin minifilaments. *J. Mol. Biol.* 143:129–145.

Schmitz, K. S. 1990. An Introduction to Dynamic Light Scattering by Macromolecules. Academic Press, New York. 449 pp.

Suzuki, N., and A. Wada. 1981. Quasielastic light scattering study of solutions of synthetic myosin filaments. *Biochim. Biophys. Acta.* 670:408–420.

Ueno, H., and W. F. Harrington. 1981. Cross-bridge movement and the conformational state of the myosin hinge in skeletal muscle. *J. Mol. Biol.* 149:619–640.